Raman Spectrum of the Phenyl Radical[#]

Andrzej Łapiński,[†,‡] Jens Spanget-Larsen,[†,‡,§] Morten Langgård,[||] Jacek Waluk,[†,‡,⊥] and J. George Radziszewski*[,†,‡]

National Renewable Energy Laboratory (NREL), 1617 Cole Blvd. Golden, Colorado 80401; Department of Chemical Engineering, Colorado School of Mines, Golden, Colorado 80401; Department of Chemistry, Roskilde University (RUC), DK-4000 Roskilde, Denmark; H. Lundbeck, DK-2500 Valby, Denmark; and Institute of Physical Chemistry, Polish Academy of Sciences, Kasprzaka 44, 01-224 Warsaw, Poland

Received: April 19, 2001; In Final Form: July 27, 2001

The Raman spectrum of phenyl radical (C_6H_5) isolated in low-temperature argon matrices has been obtained. The assignments of experimentally observed frequencies are based on comparison with results of quantum chemical calculations (B3LYP/cc-pVTZ) and with infrared absorption bands measured for $^{12}C_6H_5$ and $^{13}C_6H_5$ species. Analysis of the IR and Raman spectra, including IR linear dichroism, and of the isotopic shifts caused by $^{12}C \rightarrow {}^{13}C$ substitution allows to reconfirm most of the previous assignments and to introduce some corrections. The prominent ring breathing mode, characteristic for benzenoid compounds (991 cm^{-1} in benzene), occurs in phenyl radical at 998 cm^{-1}.

1. Introduction

Due to its role in atmospheric chemistry and, in particular, in combustion and soot formation processes,[1−4] the phenyl radical (**1**) is a very important transient intermediate. Still, its spectral structure and gas-phase reactivity remain rather poorly characterized. A consequence of the lack of available spectral information was that early kinetic studies of reactions involving phenyl radical[5−9] were based on relative rate measurements, which may lead to large errors. The measurements that yield the absolute values for the rate constants for reactions of **1** with various reagents most often employ pulse laser photolysis[10−15] or radiolysis[16] techniques. However, due to difficulties in the determination of the absorption cross sections, huge discrepancies occur in the reported rate constants, e.g., for the reaction of **1** with O_2.[10,11,15,16] Other methods that could directly probe the concentration of **1**, either in the stationary or time-resolved regime, such as luminescence or Raman spectroscopies, have not yet been employed, due to lack of data regarding emission or the vibrational structure.

In this work, we present the results of Raman spectroscopy studies of **1** and of the IR investigation of its ^{13}C isotopomer, $^{13}C_6H_5$ (**2**), both isolated in low-temperature argon matrices. Previous investigations of the vibrational spectroscopy of **1**[17−24] were based on measuring the IR absorption. The vibrational spectrum has also been calculated using HF and DFT methods.[24,25] Very recently, a detailed analysis of the infrared absorption spectrum of **1** and its five deuterated isotopomers led to assignment of all IR-active modes.[24] To our knowledge, no Raman studies have been undertaken so far. Nonresonant Raman spectroscopy of matrix-isolated larger organic intermediates is notoriously difficult due to the combination of factors: inherent weakness of the effect, low concentration of the probed species, interference of strong emissions from traces of side products or impurities, relatively low optical quality of matrices, etc. The purpose of this work is 3-fold. First, we demonstrate that the combined results of simultaneously performed matrix isolation IR and Raman measurements, IR polarization spectroscopy, and quantum theoretical calculations lead to reconfirmation of spectral assignments for most vibrational frequencies, as well as to some corrections. The latter involve transitions that are strong in Raman spectra, but weak in the IR. Second, the analysis of Raman intensities of the phenyl radical, very different from those observed for the IR transitions, may provide a basis for analytical and diagnostic applications monitoring the concentration and kinetic behavior of this important molecule. Finally, our experimental data probe the reliability of theoretical methods when it comes to the prediction of vibrational frequencies, IR intensities, and Raman scattering activities for an open-shell species.

2. Experimental Section

We employ a standard matrix isolation setup consisting of a high-vacuum station and a closed-cycle helium cryostat equipped with a vacuum shroud suited for optical spectroscopy. Two kinds of deposition targets were used in the present investigations. For IR measurements, we deposited a matrix on a BaF_2 window kept at 20 K. In Raman experiments, a platinum-coated copper plate kept at 25 K was used as a target. The flow rates varied between 0.4 and 2 mL/min in both cases. During the irradiation and spectral measurements, samples were kept at 7 K.

Various precursors can be chosen in order to obtain phenyl radicals: benzoyl peroxides,[17−20] benzoic anhydride,[23] halogenobenzenes,[26] nitrosobenzene.[21] Both pyrolytic and photolytic routes of precursor destruction lead to phenyl radicals. In this work, photodissociation of nitrosobenzene (Aldrich, 97%) or iodobenzene (Aldrich, 98%) was selected as a method of obtaining **1** and **2**. For the latter molecule, $^{13}C_6H_5I$ (Cambridge Isotope Laboratories, 99%) was chosen as a precursor. The sample of **1** was also produced by vacuum pyrolysis (at 380° C) of benzoyl peroxide (Aldrich, 97%), using the procedure

[#] Dedicated to Professor Erik W. Thulstrup on the occasion of his 60th anniversary

[†] National Renewable Energy Laboratory (NREL).

[‡] Department of Chemical Engineering, Colorado School of Mines.

[§] Department of Chemistry, Roskilde University (RUC).

[||] H. Lundbeck.

[⊥] Institute of Physical Chemistry, Polish Academy of Sciences.

10.1021/jp0114900 CCC: $20.00 © 2001 American Chemical Society
Published on Web 10/27/2001

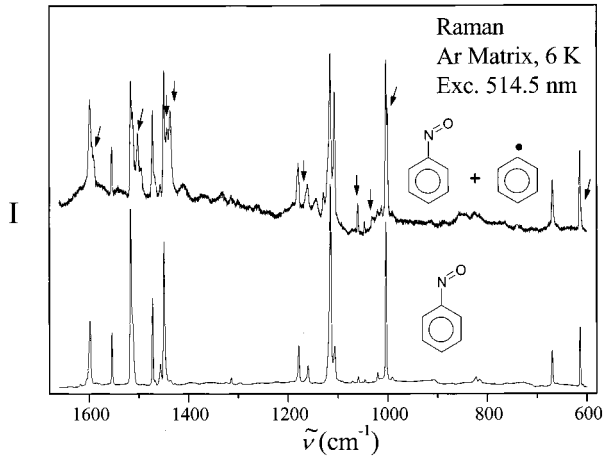

Figure 1. Raman spectrum of the nitrosobenzene isolated in Ar matrix at 6 K (bottom). Raman spectrum of the mixture of phenyl radical and nitrosobenzene (top). The excitation: 514.5 nm, Ar-ion laser, 700 mW. The top trace was obtained after prolonged excimer laser irradiation at 308 nm (3 h). The arrows mark the peaks corresponding to C_6H_5 (**1**). The mode numbers correspond to those in Table 1. The remaining peaks are due to the precursor, side products, or impurities.

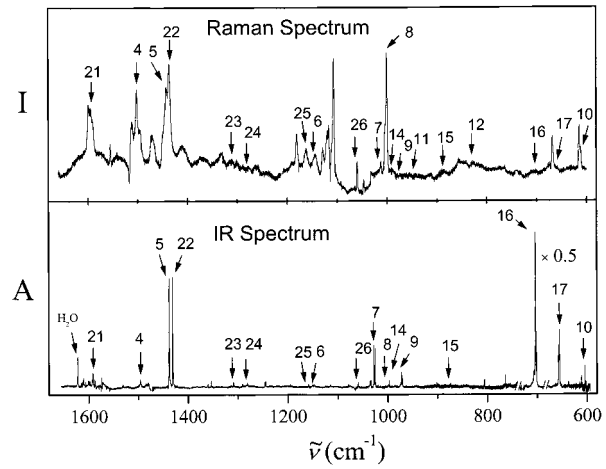

Figure 2. Comparison of the Raman (top) and IR spectra (bottom) of the phenyl radical in Ar matrix at 6 K. Raman excitation wavelength was 514.5 nm. The arrows mark the peaks corresponding to **1**. The mode numbers correspond to those in Table 1.

described in ref 24. The 308-nm line of an XeCl excimer laser (Lambda Physik Compex-102) was used for photolysis. The IR absorption spectra were recorded with a Nicolet Magna-560 FTIR instrument with resolution 0.125 cm^{-1}. Raman spectra have been collected using a Raman Spectrometer (SPEX 1403) equipped with a CCD3000 detector. The samples for Raman spectroscopy were excited using a cw-Ar-ion laser (Coherent I-308 or I-200) lines: 454.5, 488, and 514.5 nm, with the laser power on the sample ranging from 150 to 700 mW. Both 454.5 and 488 nm wavelengths are within the region of a weak $^2B_1 \leftarrow {}^2A_1$ electronic transition,[26,27] whereas the latter is slightly below the 0−0 transition energy. The scattered light was collected close to the right-angle geometry. The resolution varied between 1 and 4 cm^{-1}; the typical measurement time was 12 h.

The assignments of the vibrational transitions in **2** were reinforced by using polarized spectroscopy techniques.[28] In these experiments, both photolysis of the precursor and the photodestruction of the radical were carried out using polarized light at wavelengths for which the transition moments of the initially excited species were known. This step was followed by measurements of IR linear dichroism (LD). The signs and magnitudes of the LD for the individual bands made it possible to determine the symmetry species.[27]

The molecular equilibrium geometry and harmonic force field[29,30] for **1** and **2** were computed with the Gaussian 98 software package[31] by using B3LYP density functional theory[32,33] and the cc-pVTZ basis set.[34] IR intensities and Raman scattering activities for the fundamental vibrational transitions of phenyl and its isotopomers were computed by using standard procedures (freq=raman) and default parameters.[31]

3. Results

Irradiation of nitrosobenzene isolated in an argon matrix with a 308 nm line leads to its decomposition and to the formation of the phenyl radical. This is shown in Figure 1, where we present the initial IR spectrum of nitrosobenzene along with the Raman spectrum of a partially photolyzed sample. The identification of bands belonging to the phenyl radical was based on the results of multiple experiments, described in detail in a recent papers.[24,27] These experiments involved (i) gradual photolytic destruction of the precursor and the ensuing phenyl radical, accompanied by monitoring of the IR absorption growth and decay simultaneously with Raman or UV−Vis absorption[27] measurements; (ii) use of several precursors; (iii) recording spectral changes occurring during sample annealing, in particular observation of formation of biphenyl (for phenyl radical generated from diphenyl peroxide) or regeneration of nitroso- or iodobenzene (for samples containing phenyl radical prepared from these precursors); (iv) isotopic substitution; and (v) polarization studies. Combination of all these procedures allowed us to separate spectral features due to precursors, various photolysis products and the impurities from those assigned to **1**.

The destruction of the precursor leads to the IR spectrum shown in Figure 2. The same drawing shows the Raman spectrum. One can immediately notice completely different intensity patterns. For instance, the line at 703 cm^{-1}, most intense in the IR, is barely visible in the Raman spectrum. On the contrary, the strongest Raman transitions observed at 998 cm^{-1}, corresponds to a very weak IR band. Similar is the case with the lines at 1497 and 1593 cm^{-1}, which are much more intense in the Raman spectrum. The only two transitions that are quite strong in both IR and Raman spectra are detected at 1432 and 1439 cm^{-1}.

We have also measured the IR spectrum of **2**, a fully ^{13}C-substituted species, obtained after photolysis of the iodobenzene precursor. Comparison of the IR spectra of **1** and **2** is shown in Figure 3. The values of experimentally detected and calculated infrared transitions for **1** and **2** are presented in Table 1.

4. Discussion

Among the 27 fundamental vibrations of **1**, 24 are active in the IR ($10\mathbf{a_1} + 5\mathbf{b_1} + 9\mathbf{b_2}$). All 27 vibrations should be Raman-active. However, very low intensities are predicted by theory for many bands, in particular those corresponding to $\mathbf{a}_2$ and $\mathbf{b}_1$ transitions. This is in line with our observations. All the most intense Raman transitions that we detect correspond to $\mathbf{a_1}$ and $\mathbf{b_2}$ symmetry species (Table 1). The lines corresponding to $\mathbf{b}_1$ species are much weaker. Finally, we do observe weak Raman lines at 946 cm^{-1} and 816 cm^{-1}. Because these bands are not detected in the IR spectrum, we tentatively assign them to $\mathbf{a_2}$ transitions, calculated to lie at 972 and 819 cm^{-1}, respectively.

In general, our results are in very good agreement with a recently published work on the IR spectrum of **1**.[24] The

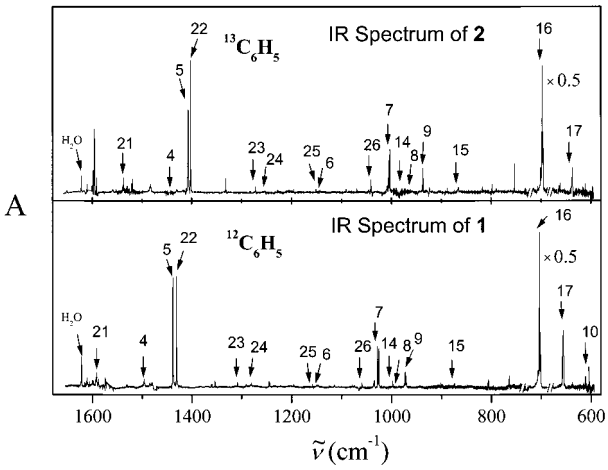

Figure 3. Comparison of the IR spectra of C_6H_5 (**1**) (bottom) and $^{13}C_6H_5$ (**2**) (top). The arrows mark the peaks corresponding to **1** and **2**. The mode numbers correspond to those in Table 1.

discrepancy arises concerning the region around 1500−1600 cm^{-1}. Previous work assigned a band at 1581 cm^{-1} to an $\mathbf{a_1}$ species and a band at 1624 cm^{-1}, to a $\mathbf{b_2}$ transition. Our results show that latter band is not due to phenyl radical because it cannot be obtained with the same relative intensity from all precursors. Always present, in these experiments, traces of water have in Ar matrices absorption at 1624 cm^{-1}, as it can be seen in Figure 3. We observe two strong Raman transitions at 1497 and 1593 cm^{-1} that we assign to $\mathbf{a_1}$ and $\mathbf{b_2}$ species, respectively. Without the help of Raman spectroscopy and ^{13}C labeling these transitions would have been difficult to assign, due to weak IR intensities and to spectral overlap with bands of the precursor and water.

Our assignments for **1** are nicely confirmed by the results obtained for **2**, the ^{13}C-substituted species. ^{12}C → ^{13}C replacement produces spectral shifts, but does not lead to a change in the overall pattern of the spectrum. The spectral shifts vary from 5 to 55 cm^{-1}; the analysis of their values greatly facilitates the assignments. For instance, two close-lying transitions of $\mathbf{b_2}$ symmetry are observed in **1** at 1310 and 1281 cm^{-1}. In **2**, these bands shift to 1273 and 1262 cm^{-1}. The theory predicts two $\mathbf{b_2}$ transitions in this region, calculated for **1** at 1327 and 1305 cm^{-1}, respectively. The computed frequency shifts for these two transitions are 21 and 36 cm^{-1}. The only way these shifts are compatible with experiment is when the transition calculated at higher energy is assigned to the one experimentally observed at lower energy, and vice versa. Within this assignment, the experimental shifts of 37 and 18 cm^{-1} are in excellent agreement with the computed values of 36 and 21 cm^{-1}.

Comparison between predicted and observed Raman spectra is shown in Figures 4−6. The overall agreement is very satisfying, albeit the standard deviations, 14 cm^{-1} for **1** and 12 cm^{-1} for **2**, are larger than the value obtained for benzene, 4 cm^{-1}. For nearly all vibrations, the value of the ratio of calculated to experimental values is practically constant (1.03 ± 0.01). The computed shifts accompanying ^{12}C → ^{13}C substitution are in excellent agreement with observed values, which provides yet another argument confirming the spectral assignments. The least reliable predictions concern the Raman intensities, in particular in the region 1000−1500 cm^{-1}. Although the agreement with theory is good for the three strong Raman bands at 998, 1497, and 1593 cm^{-1}, this is not the case with the two strong bands at 1439 and 1432 cm^{-1}, and with a weak band at 1151 cm^{-1}. It should be noted, however, that the calculations do not take into account possible resonance or

TABLE 1: Experimental and Calculated Vibrational Transitions for 1 and 2: $\tilde{\nu}$ = Wavenumber (cm^{-1}), I = IR Intensity (km/mol), A = Raman Scattering Activity (Å^4/amu), Δ = Isotopic Wavenumber Shift (cm^{-1})

	C_6H_5						$^{13}C_6H_5$							
	exptl[a]			calcd[b]			exptl[a]			calcd[b]				
sym	$\tilde{\nu}$	I[d]	A	$\tilde{\nu}$	I	A	$\tilde{\nu}$	Δ	I	$\tilde{\nu}$	Δ	I	A	mode description[c]
1 $\mathbf{a_1}$	3086	6.1	w	3188	10.4	307.2				3177	11	10.5	306.6	CH s str
2	3072	1.9	w	3175	4.3	148.0				3165	10	4.2	152.8	*o,p*-CH str
3	3037	0.8	w	3156	1.0	23.4				3147	9	1.0	24.0	CH str
4	1497	vw	s	1574	0.6	6.9	1447	50	vw	1523	51	0.2	6.4	$C_{2,5}$−$C_{3,6}$ s str $C_{3,5}$−H ip b
5	1439	8.6	s	1476	8.7	1.9	1408	31	6.4	1443	33	9.9	2.4	C_1−$C_{2,6}$ s str $C_{2,3,5,6}$−H ip b
6	1151	0.8	w	1178	0.1	8.4	1143	8	0.4	1171	7	0.1	7.7	*o,m*-CH ip b
7	1028	6.5	w	1052	7.9	3.2	1005	23	3.5	1030	22	7.5	0.8	$C_{2,3,5,6}$−H ip b
8	998	0.1	s	1019	0.3	52.4	960	38	0.1	983	36	0.0	49.5	ring breathing
9	973	0.7		995	1.5	1.0	937	36	2.2	958	37	1.1	1.5	ring b
10	605	0.5		621	1.7	4.5	582	21	1.1	598	23	1.6	4.2	ring b
11 $\mathbf{a_2}$	945[e]		vw	972	0.0	0.0				961	11	0.0	0.0	$C_{2,3,5,6}$−H oop b
12	816[e]		vw	819	0	0.6				812	7	0.0	0.8	$C_{2,3,5,6}$−H oop b
13				403	0.0	0.0				392	11	0.0	0.0	$C_{2,3,5,6}$−H oop b
14 $\mathbf{b_1}$	990	0.1	w	1002	0.2	0.0	982	8	0.1	992	10	0.2	0.0	oop ring b; *m,p*-CH oop b
15	873	0.1	w	900	0.4	0.4	866	7	0.1	891	9	0.4	0.4	*o,p*-CH oop b
16	703	32.0	vw	726	65.7	0.0	697	6	43.2	719	7	76.1	0.0	C−H oop b
17	655	8.1	vw	679	23.6	0.8	637	18	2.6	660	19	13.4	0.8	*o,p*-CH oop b
18	415	4.3	w	429	6.3	0.2	402	13	4.2	416	13	5.5	0.2	$C_{2,3,5,6}$−H oop b; oop ring b
19 $\mathbf{b_2}$	3070	3.4	w	3177	21.7	1.7				3167	10	21.2	2.3	*o,m*-CH str
20	3060	1.4	w	3162	3.4	145.0				3153	3	3.7	145.3	*o,m*-CH str
21	1593	1.6	m	1630	2.1	10.1	1538	55	1.6	1571	59	2.2	9.8	CC str
22	1432	5.3	s	1468	6.0	0.4	1403	29	3.8	1438	30	6.1	0.3	*m,p*-CH ip b
23	1310	0.1	w	1305	0.4	0.2	1273	37	0.1	1269	36	0.6	0.0	$C_{2,5}$−H ip b; Kekulé mode
24	1281	0.2	w	1327	0.1	1.3	1262	18	0.3	1306	21	0.0	1.5	*m,p*-CH ip b
25	1159	0.1	w	1178	0.2	1.2	1154	5	0.1	1171	7	0.2	0.9	*m,p*-CH ip b
26	1060	3.4	w	1074	3.4	1.2	1041	19	0.8	1055	19	2.8	1.1	$C_{2,5}$−$C_{3,6}$ str; $C_{3,4,5}$−H ip b
27	588	0.2	w	602	0.6	3.6	567	21	0.7	580	22	0.5	3.3	ring b

[a] Argon matrix, iodobenzene precursor. [b] UB3LYP/cc-pVTZ (unscaled). [c] Approximate mode description: str = stretch, s = symmetric, as = asymmetric, b = bend, ip = in-plane, oop = out of plane. [d] See ref 35 for experimental determination of absolute IR intensities. [e] Observed only in the Raman spectrum, tentative assignment.

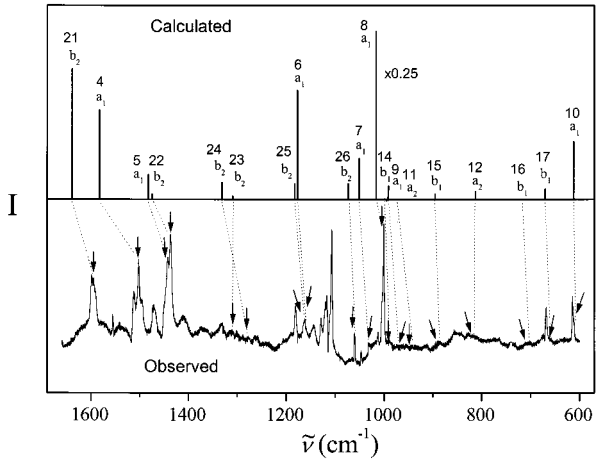

Figure 4. Observed (bottom) and calculated (top) Raman spectra of the phenyl radical. The arrows mark the peaks corresponding to **1**. See Table 1 for mode numbers.

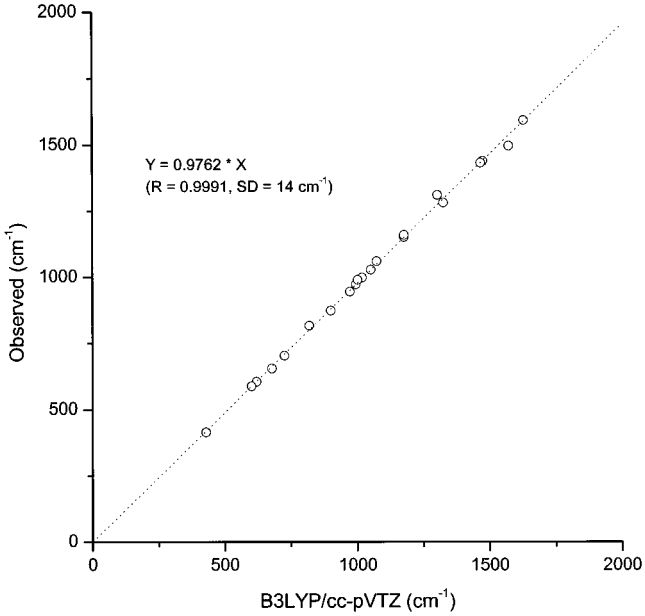

Figure 5. Correlation between the observed and calculated frequencies for C_6H_5 (**1**).

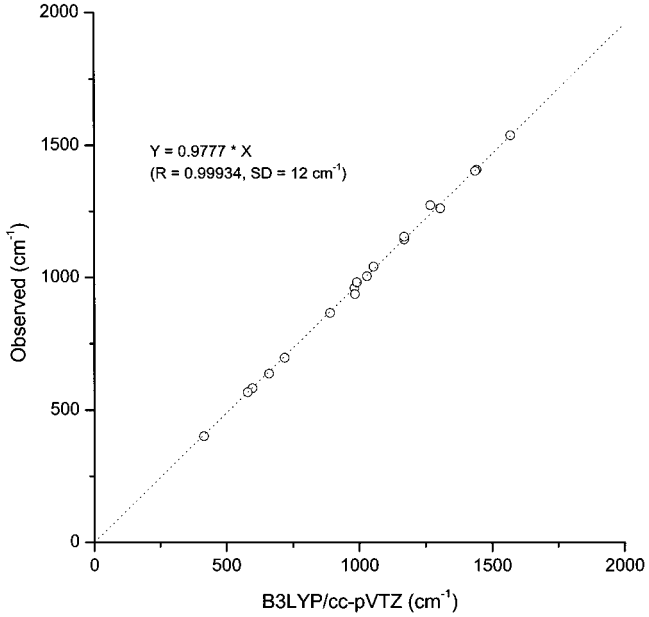

Figure 6. Correlation between the observed and calculated frequencies for $^{13}C_6H_5$ (**2**).

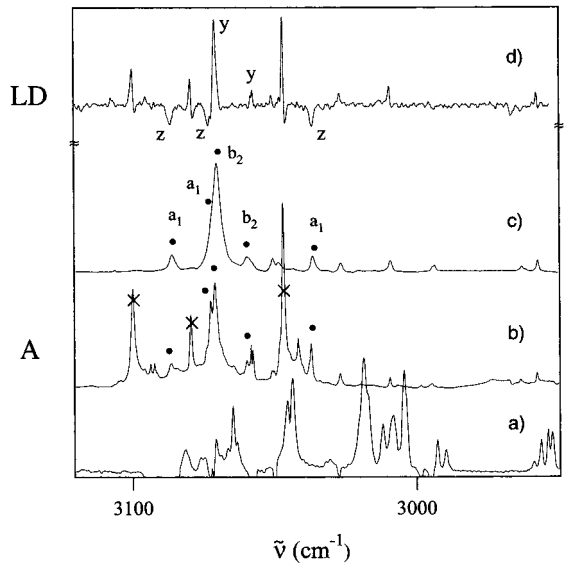

Figure 7. C−H stretching region of IR absorption of C_6H_5 (**1**): (a) obtained in an Ar matrix after photolysis of iodobenzene; (b) obtained from vacuum pyrolysis of benzoyl peroxide; (c) measured after photolysis of nitrosobenzene. Curve (d) shows linear dichroism spectrum determined after partial photobleaching of **1**, with vertically polarized 248 nm light (irradiation into the $^2A_1$ state of **1**). LD denotes the difference in absorption measured along and perpendicular to the vertical direction.

preresonance effects due to the fact that the wavenumbers of the laser lines used for measuring the Raman lie in the vicinity of the energy of the lowest excited doublet state of **1**.

Comparing the results obtained from different precursors, we have observed that the IR spectra of **1** and **2** produced by photolysis of iodobenzene are most complex. For several vibrations, line splittings are observed. A dramatic difference between the spectra of the species obtained from iodobenzene and those from other precursors occurs in the region of C−H stretching vibrations. Figure 7 shows the spectra taken in this spectral region for the samples of **1** obtained from photolysis of iodobenzene and nitrosobenzene, and from pyrolysis of benzoyl peroxide. Included is also a linear dichroim (LD) spectrum, obtained after partial destruction of **1** with light polarized along the C_2 molecular axis. Analysis of the LD spectrum makes it possible to separate the bands belonging to **1** from those due to precursors or impurities, and to determine polarizations of vibrational transitions.[27] For instance, photobleaching of **1** by irradiation into a transition polarized along the symmetry axis should lead to a negative LD signal for $\mathbf{a_1}$ transitions, and to a positive signal for $\mathbf{b_2}$ transitions. The LD analysis is feasible for **1** produced by nitrosobenzene photolysis and by benzoyl peroxide pyrolysis, followed by partial photobleaching of **1**. However, when iodobenzene is used as precursor, the lines are shifted and split into several components, hampering the assignments. Because iodobenzene was the only precursor used for the generation of **2**, this is the reason no frequencies for the CH stretching vibrations are given for this species in Table 1.

We believe these complications arise from the fact that the iodine atoms produced as a result of photolysis remain in close proximity to the phenyl radical. Actually, it has been observed that after photolysis of nitrosobenzene, triplet radical pairs are generated. They were detected and characterized by ESR

spectroscopy.[21] Two distinct values for the average separation distance were found, corresponding to two different positions of NO with respect to **1**. Hence, it may be expected that the vibrational structure of **1** produced by photolysis of iodobenzene can "feel" various locations of the iodine atom with respect to both distance and orientation. It seems natural that the vibrations mostly affected are those corresponding to C−H stretches, since the motion of hydrogen atoms probes the most outward portion of space around the phenyl radical.

5. Conclusions

Most of the Raman-active modes of **1** were observed and assigned under conditions of matrix isolation in argon. IR spectra were also measured for the $^{13}C_6H_5$ radical. The observed spectral shifts, and their perfect agreement with computed values ensured the reliability of the assignments of the vibrational transitions for **2**, reinforced the previous interpretations for **1** and led to some refinement of previous assignments. The Raman and IR intensity patterns are very different, showing that the mutual exclusion principle, strict for the parent, centrosymmetric benzene molecule, holds approximately in the phenyl radical. The observed strong Raman transitions provide "fingerprint" frequencies that can be used for analytical purposes.

Acknowledgment. J.G.R. is grateful for generous financial support from the NREL FIRST and DDRD programs. Experimental work was supported in part by DURIP Grant No. F49620-99-1-0150 and funds from CSM. Encouragement and support by Dr. Gene Peterson (NREL) is also acknowledged.

References and Notes

(1) Haynes, D. S. In *Fossil Fuel Combustion*; Wiley-Interscience: New York, 1991, p 261.
(2) Bockhorn, H. *Soot Formation in Combustion*; Springer-Verlag: New York, 1993.
(3) Glassman, I. *Combustion*, 2nd ed; Academic Press: New York, 1986.
(4) Violi, A.; D'Anna, A.; D'Alessio, A. *Chem. Eng. Sci.* **1999**, *54*, 3433.
(5) Fielding, W.; Pritchard, H. O. *J. Phys. Chem.* **1962**, *66*, 821.
(6) Duncan, F. J.; Trotman-Dickenson, A. F. J. *J. Chem. Soc.* **1962**, 4672.
(7) Kerr, J. A.; Moss, S. J. *Handbook of Bimolecular and Termolecular Gas Reactions*; CRC Press: Boca Raton, FL, 1981, vol. 1.
(8) Fahr, A.; Stein, S. E. *22nd Symp. Int. on Combustion [Proceedings]*; The Combustion Institute: Pittsburgh, PA, 1988, p 1023.
(9) Fahr, A.; Mallard, W. G.; Stein, S. E. *21st Symp. Int. on Combustion [Proceedings]*; The combustion Institute, Pittsburgh, PA, 1986, p 825.
(10) Preidel, M.; Zellner, R. *Ber. Bunsen-Ges. Phys. Chem*. **1989**, *93*, 1417.
(11) Yu, T.; Lin, M. C. *J. Am. Chem. Soc.* **1993**, *115*, 4371; Yu, T.; Lin, M. C. *J. Am. Chem. Soc.* **1994**, *116*, 9571;
(12) Yu, T.; Lin, M. C. *J. Phys. Chem.* **1994**, *98*, 2105.
(13) Park, J.; Lin, M. C. *J. Phys. Chem. A* **1997**, *101*, 14.
(14) Park, J.; Burova, S.; Rodgers, A. S.; Lin, M. C. *J. Phys. Chem. A* **1999**, *103*, 9036.
(15) Sommeling, P. M.; Mulder, P.; Low, R.; Atila, D. V.; Lusztyk, J.; Ingold, K. U. *J. Phys. Chem.* **1993**, *97*, 8361.
(16) Wallington, T. J.; Egsgaard, H.; Nielsen, O. J.; Platz, J.; Sehested, J.; Stein, T. *Chem. Phys. Lett.* **1998**, *290*, 363.
(17) Packansky, J.; Bargon, J. *J. Am. Chem. Soc.* **1975**, *97*, 6896.
(18) Packansky, J.; Gardini, G. P.; Bargon, J. *J. Am. Chem. Soc.* **1976**, *98*, 2655.
(19) Packansky, J.; Brown, D. W. *J. Phys. Chem.* **1983**, *87*, 1553.
(20) Jacox, M. E. *J. Phys. Chem.* **1982**, *86*, 670.
(21) Hatton, W. G.; Hacker, N. P.; Kasai, P. H. *J. Chem. Soc., Chem. Commun.* **1990**, 227.
(22) Gunion, R.; Gilles, M.; Polak, M.; Lineberger, W. C. *Int. J. Mass Spectrom. Ion. Proc.* **1992**, *117*, 621.
(23) Radziszewski, J. G.; Nimlos, M. R.; Winter, P. R.; Ellison, G. B. *J. Am. Chem. Soc*. **1996**, *118*, 7400.
(24) Friderichsen, A. V.; Radziszewski, J. G.; Nimlos, M. R.; Winter, P. R.; Dayton, D. C.; David, D. E.; Ellison, G. B. *J. Am. Chem. Soc.* **2001**, *123*, 1977.
(25) Huang, J.-H.; Han, K.-L.; Zhu, R.-S.; He, G.-Z. *Spectrochim. Acta A* **1999**, *55*, 1165.
(26) Porter, G.; Ward, B. *Proc. R. Soc. London Ser. A* **1965**, *287*, 457.
(27) Radziszewski, J. G. *Chem. Phys. Lett.* **1999**, *301*, 565.
(28) Michl, J.; Thulstrup, E. W. *Spectroscopy with Polarized Light. Solute Alignment by Photoselection, in Liquid Crystals, Polymers, and Membranes*; VCH Publishers Inc.: New York, 1986.
(29) Foresman, J. B.; Frisch, Æ. *Exploring Chemistry with Electronic Structure Methods*; Gaussian, Inc.: Pittsburgh, PA, 1996.
(30) Jensen, F. *Introduction to Computational Chemistry*; Wiley: Chichester, 1999.
(31) Frisch, M. J.; Trucks, G. W.; Schlegel, H. B.; Scuseria, G. E.; Robb, M. A.; Cheeseman, J. R.; Zakrzewski, V. G.; Montgomery, J. A., Jr.; Stratmann, R. E.; Burant, J. C.; Dapprich, S.; Millam, J. M.; Daniels, A. D.; Kudin, K. N.; Strain, M. C.; Farkas, O.; Tomasi, J.; Barone, V.; Cossi, M.; Cammi, R.; Mennucci, B.; Pomelli, C.; Adamo, C.; Clifford, S.; Ochterski, J.; Petersson, G. A.; Ayala, P. Y.; Cui, Q.; Morokuma, K.; Malick, D. K.; Rabuck, A. D.; Raghavachari, K.; Foresman, J. B.; Cioslowski, J.; Ortiz, J. V.; Stefanov, B. B.; Liu, G.; Liashenko, A.; Piskorz, P.; Komaromi, I.; Gomperts, R.; Martin, R. L.; Fox, D. J.; Keith, T.; Al-Laham, M. A.; Peng, C. Y.; Nanayakkara, A.; Gonzalez, C.; Challacombe, M.; Gill, P. M. W.; Johnson, B. G.; Chen, W.; Wong, M. W.; Andres, J. L.; Head-Gordon, M.; Replogle, E. S.; Pople, J. A. *Gaussian 98*, revision A.3; Gaussian, Inc.: Pittsburgh, PA, 1998.
(32) Becke, A. D. *J. Chem. Phys.* **1993**, *98*, 5648.
(33) Lee, C.; Yang, W.; Parr, R. G. *Phys. Rev. B* **1988**, *37*, 875.
(34) Dunning, T. H., Jr. *J. Chem. Phys*. **1989**, *90*, 1007. Kendall, R. A.; Dunning, T. H., Jr.; Harrison, R. J. *J. Chem. Phys.* **1992**, *96*, 6796. Wilson, A. K.; van Mourik, T.; Dunning, T. H., Jr. *J. Mol. Struct.* **1996**, *388*, 339.
(35) Radziszewski, J. G.; Hess, B. A., Jr.; Zahradník, R. *J. Am. Chem. Soc*. **1992**, *114*, 52.